

X-621-64-281

**NASA-TMX-55117**

PO PRICE \$ \_\_\_\_\_

OTS PRICE(S) \$ \_\_\_\_\_

Hard copy (HC) 1.60Microfiche (MF) 1.50

# TELEMETRY INSTRUMENTATION OF THE ECHO II PASSIVE COMMUNICATIONS SATELLITE

BY  
**HAROLD S. HORIUCHI**

N65 15657

ACCESSION NUMBER

13

TMX 55117

NASA CR OR TMX OR AD NUMBER

(THRU)

3

(CODE)

07

(CATEGORY)

OCTOBER 1964

FACILITY 1 2 3 4 5 6 7 8 9 10



**GODDARD SPACE FLIGHT CENTER**  
**GREENBELT, MARYLAND**

Paper was presented at the 8th International Convention on Military Electronics  
MIL-E-CON 8 in Washington, D. C., September 14-16, 1964

TELEMETRY INSTRUMENTATION  
OF THE ECHO II  
PASSIVE COMMUNICATIONS SATELLITE

by  
Harold S. Horiuchi

October 1964

Goddard Space Flight Center  
Greenbelt, Maryland

## TELEMETRY INSTRUMENTATION OF THE ECHO II PASSIVE COMMUNICATIONS SATELLITE

By

Harold S. Horiuchi  
Goddard Space Flight Center  
Greenbelt, Maryland

The beacon telemetry system used on the Echo II satellite was to provide a tracking signal and to monitor the skin temperature and measure the internal pressure of the satellite, with particular emphasis on data acquisition during the initial inflation stages. A faithful TM system having very sensitive sensors with very short time constants was required since the inflation of the balloon (the satellite) was to take place in a matter of minutes.

In addition to the data acquisition requirement, there were the inevitable environmental and physical requirements that had to be satisfied. First of all, the size was limited by the space available in the overall payload package. The weight of the beacon system was also limited because of overall weight limit of the payload package and the concentrated mass of the beacons themselves.

The telemetry beacon that was finally designed, constructed and flown was packaged into a square, flat pancake, 14 inches square by  $3/4$  inch thick. It weighed approximately 3 pounds of which almost half was accounted for by the two battery packs. The solar modules consisted of four triangular pancakes weighing approximately  $3/4$  pound each. The total weight of a complete beacon system weighed just under six pounds. There were two of these systems on board the Echo II. The 12 pounds of electronic gear amounted to only two per cent of the total payload.



Figure 1. Attaching Beacon



Figure 2. Solar Panels



Figure 3. Folded Sphere

Figure 1 shows the beacon being attached to the skin of the satellite with pressure sensitive adhesive and tapes. Figure 2 shows a better view of the solar panels in place. Figure 3 shows the balloon folded into the bottom half of the canister. A plastic enclosure will be placed over this package and the air evacuated to reduce the height of the folded balloon so that the top half of the canister can be put into place.

Figure 4 is a schematic of the folded balloon packaged into the payload canister.

Upon injection of the spacecraft into the orbital path, the canister opens and the folded sphere is released. It expands partially due to the residual air within the folds; later it is stressed into a rigidized sphere by means of the controlled inflation system consisting of a number of bags of a subliming material mounted strategically inside the folded balloon.

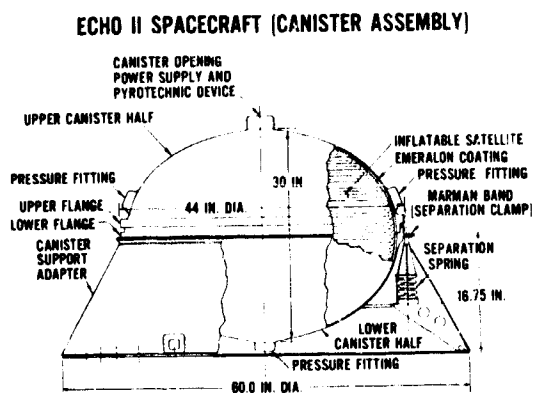


Figure 4



Figure 5. Inflated Echo II

Figure 5 shows a fully inflated Echo II. The photo was taken during the static inflation test held in the summer of 1963 in the famous dirigible hangar at the Lakehurst Naval Air Station, New Jersey.

Data wise, the beacons were required to sense balloon skin temperatures which were expected to vary anywhere between minus 120 degrees Centigrade and plus 160 degrees, a tremendous range to be covered. The internal pressure to be monitored was expected to range from a minimum of  $10^{-5}$  mm of Hg to 0.5 mm of Hg under the expected orbital conditions. The five orders of magnitude of pressure range monitoring was also a tough requirement. Time does not permit a detailed discussion of the specific electrical, mechanical and environmental requirements and tests. (References 2, 3 and 4) Those interested may obtain this information from the Project Echo Office at the Goddard Space Flight Center. However, some interesting applications of circuits and schemes employed will be briefly described later.

Figure 6 is a block diagram of the telemetry beacon employed. Basically, the system consisted of two redundant amplitude modulated transistorized RF transmitters operating at the Minitrack frequencies of 136.020 and 136.170 megacycles, respectively. The effective radiated

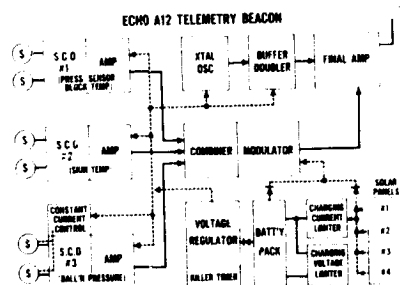


Figure 6

RF power of the two beacons was approximately 35-39 milliwatts each. Each transmitter consists of a crystal oscillator working at 68 megacycles on the fifth harmonic of a 13.6 Mc quartz crystal, followed by a frequency doubler-buffer stage and the final amplifier. Tight restrictions on the stability of the carrier frequency made the design effort extremely difficult, especially in view of the fact that temperature control of the crystal oscillator was precluded by space, weight, and other limitations. It is interesting to note, however, that a doppler frequency check was made on one of the beacons three months after launch and the carrier was found to have shifted only about 250 cycles from the last prelaunch check made a month before the actual launch. It will be noted that the specifications allowed a plus or minus 0.002 percent drift or a maximum of 2,600 cycles. During the three months in flight the beacons had gone through a complete cycle of extreme environmental temperatures and had been turned on and off at periodic intervals of about 100 seconds during this time.

Because of the extreme stability required, all of the circuits except the series modulator operated from a regulated voltage supply (See Figure 6). The dotted lines show the power connections. The solid lines indicate the signal paths. The modulator contained a waveform control circuit which employed its own feedback system and consequently had its own regulation system.

Because of the size and weight limitations again, the battery packs were limited to a total of 16 (8 each) nickel-cadmium cells with a maximum voltage of 21 volts and a capacity of 600 milliampere hours when fully charged. The regulated output was to be held at 19.2 volts by design. The four solar panels were in parallel and were to charge the batteries through a current limiting circuit whenever any solar panel

voltage rose above 22 volts. The maximum voltage output from the solar panels was expected to be around 30 volts with a total power capacity of 16 watts. The beacon power requirement was only 2.8 watts including the battery charging requirement. A string of zener diodes was placed across the batteries to hold the charging voltage to approximately 24 volts to prevent damage to the batteries during the charging cycles. The solar panels were also placed in the overall circuitry such as to power the beacon in the event of battery rundown or failure.

The temperature and pressure data were to be covered through subcarrier channels, which were fed into a combiner-modulator stage. The three subcarrier circuits were essentially identical despite the different types of information to be conveyed. The subcarrier oscillators are of the Wien bridge type employing matched thermistors for frequency control.

Figure 7 shows both the Wien bridge circuit and the beacon subcarrier oscillators. The conventional Wien bridge employs a RC circuit with capacitors in the two bridge arms being ganged and variable. In the Echo beacon the resistance elements were used as the frequency control. Since it was impossible to gang the thermosensitive elements mechanically, the thermistors were carefully matched for the nominal resistance values and temperature coefficients. Instead of employing a lamp type degeneration for output control, a feedback system was employed.

The pressure sensing, however, was slightly more involved. Here a scheme similar to the Hasting airflow gage was used but using fine thermistor beads instead of thermopiles. The design for an accurate low pressure measurement was first suggested by Ainsworth and Flanick (Reference 1) of the Goddard Space Flight Center.

Figure 8 is an attempt to illustrate in a simplified manner the temperature sensor assembly and mounting. The thermistors were mounted

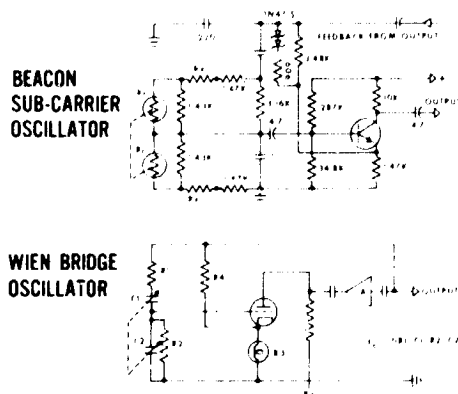


Figure 7

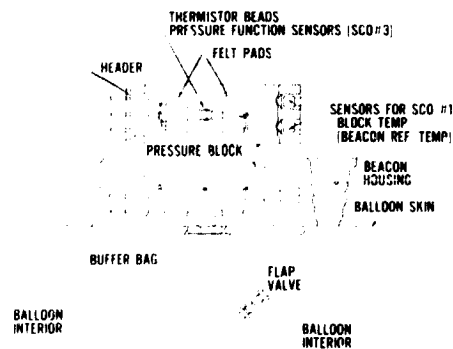


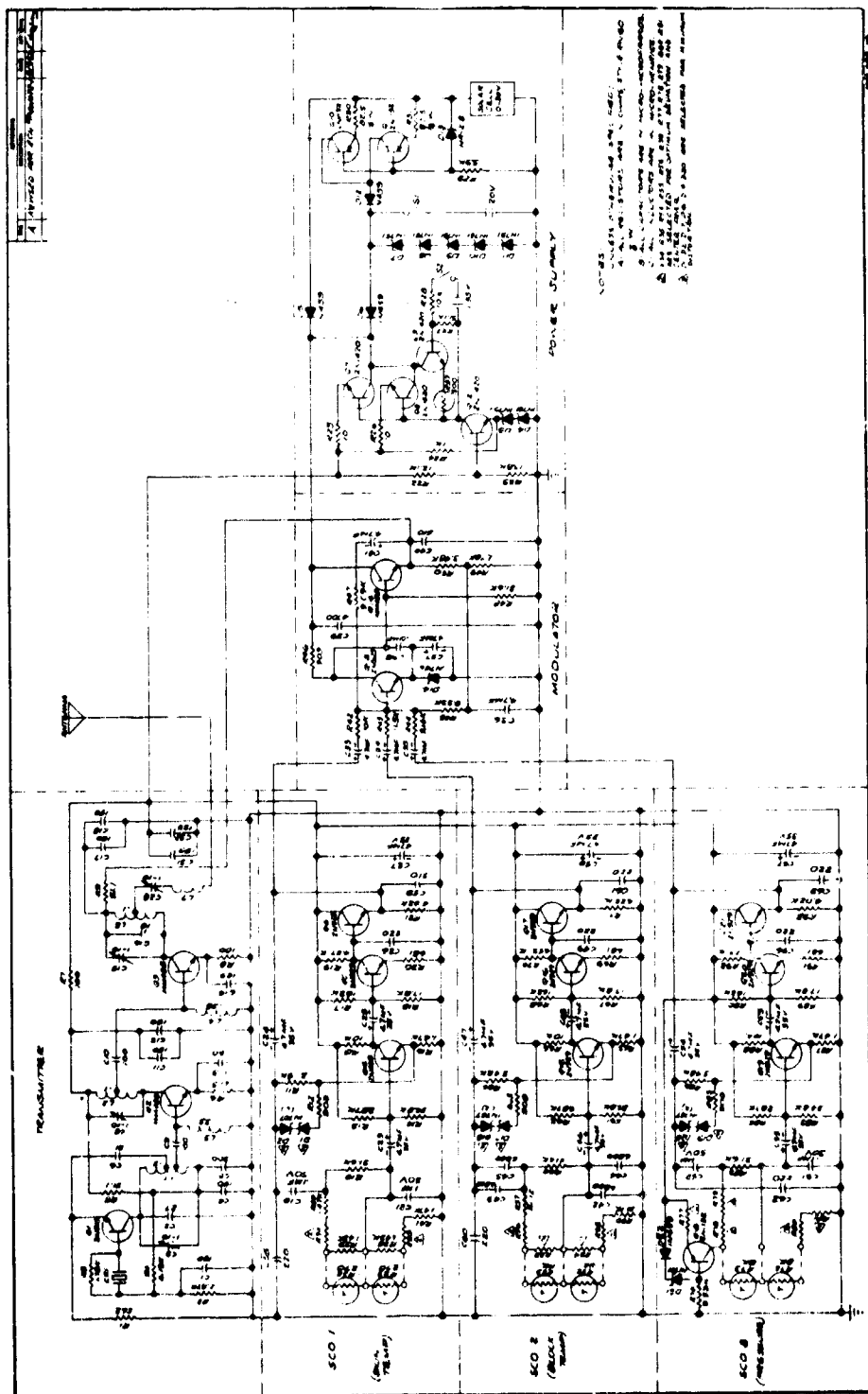
Figure 8

in a metallic cavity with a small opening exposed to the gas being monitored. The opening was protected by a radiation shield to prevent the effect of direct heat radiation from affecting the thermistor temperature. Space does not permit a detailed discussion of the principles. Bombardment of the thermistors in the cavity by the gas molecules lowers the thermistor temperature and hence the resistance and the oscillator frequency. The higher the pressure the greater the molecular activity of the gas particles and the greater probability of collision with thermistors and hence the cooling effect.

Since reference temperature was required with this type of a sensing system, the thermistors in the bridge circuit were kept at a higher temperature than the anticipated balloon gas temperature by passing a constant dc current, taken from the regulated supply line, through the thermistors. The reference temperature was monitored by sensing the temperature of the cavity block.

Calibration of both the temperature and pressure sensors posed a problem in that relatively wide range of temperature and pressures had to be monitored. Fortunately, it was possible to select thermistors with proper temperature coefficients and by using appropriate trimming resistances, it was possible to fit the data coverage into the allotted telemetry channels. Figure 9 illustrates the entire schematic diagram





of the beacon circuitry. Figure 10 shows a typical calibration curve for the skin temperature sensor. Note three curves almost parallel to each other, indicating the temperature sensitivity of the subcarrier. In this case, the dependence is very slight. One can also see the wide range of temperature squeezed into a narrow range of the subcarrier channel (IRIG 3).

Since the pressure sensor subcarrier was also temperature sensitive, only more so, the third subcarrier (IRIG 2) was used to monitor the temperature of the pressure sensor cavity block for calibration reference. Figure 11 illustrates a typical block temperature calibration curve. Since the entire beacon was potted with foam plastic and engineering tests had indicated that the temperature rise of the beacon under continuous operation was not greater than 25 degrees Centigrade, the calibration range of the reference temperature was limited to 70 degrees, from minus 10 to plus 60 degrees Centigrade covered within a subcarrier frequency range of 80 cycles. During the approximately six months that the beacons have been monitored to date, the reference block temperature has not been lower than minus 10 degrees nor higher than 30 degrees. The mean block temperature has ranged between 15 and 20 degrees. In this temperature region the slope is essentially linear which simplified the interpolation of the skin temperature and pressure.

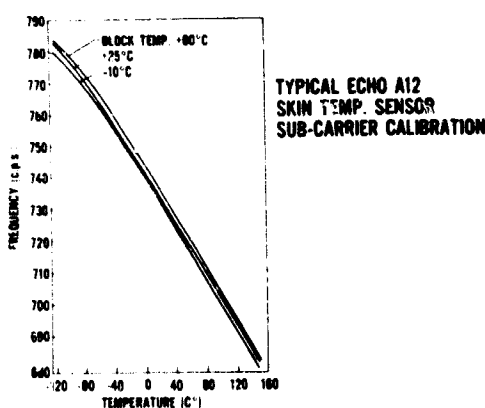


Figure 10

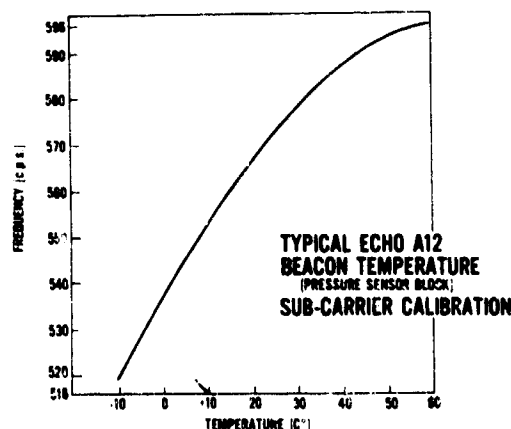


Figure 11

The extreme block temperatures were encountered only during the deepest eclipse and maximum sunlight periods.

The calibration of the pressure sensor posed other problems in addition to the wide range to be covered. First was the question of calibration with the actual gas to be used in the inflation system. Since there were several possible choices of the inflation material, a scheme that would be compatible to all of the possible materials was required.

Figure 8 also shows the over pressure sensing scheme. It was decided to calibrate the sensors with air using a buffer chamber between the sensor and the main chamber...the balloon. The buffer bag became a part of the balloon, and consisted of a tetrahedron shaped polyethylene bag into which the pressure sensor "looked" through the cavity opening. A small one way pressure release valve was provided on the buffer chamber for pressure equalization as the balloon pressure increased during the inflation process; this valve was primarily for monitoring the decreasing balloon pressure.

Figure 12 is a typical pressure calibration chart. One can see the heavy dependence of the calibration curves on the block or the beacon reference temperature.

Figure 13 shows how the pressure and temperature read during the initial inflation stage of the Echo satellite. The chart represents data for two orbits or about three and half hours of flight after deployment. Dotted portions of the curves have been approximated and represent data missing owing to the separation distance between the tracking stations, which precluded a continuous orbital coverage.

The internal pressure has long since been dissipated. The temperatures of the skin and of the beacon, however, continue to be monitored and they reflect the mean values as the respective sensors rotate about a yet to be determined spin axis of the satellite. Skin temperatures as

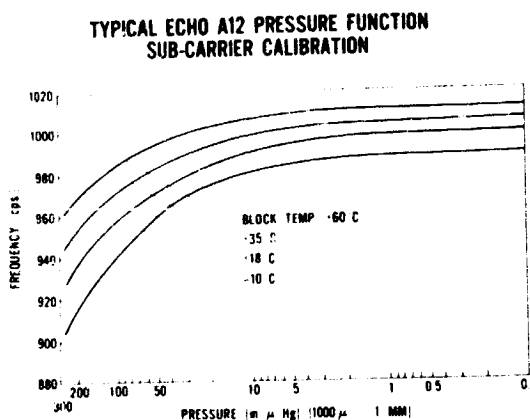


Figure 12

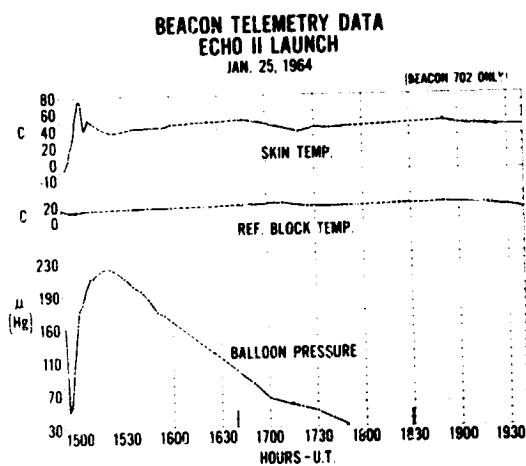


Figure 13

high as 90 degrees Centigrade have been recorded at times. The lowest temperature recorded was minus 115 degrees just moments after the satellite emerged from the earth's shadow and the beacon turned on. Minus 115°C. is just about the lower limit of the sub-carrier calibration. The average skin temperature of the Echo II during the past six months in orbit has been about 50 degrees Centigrade.

The telemetry beacons have provided certain other information not originally intended to be obtained. One of considerable interest in many quarters is the rotation speed of the satellite. Another is the location of the spin axis on the satellite and its attitude. One finds that the rotation period has been varying during the past six months; the variations have been very slight however. Figure 14 shows the

rotation period in seconds plotted versus time in increments of 10 orbits. The orbit numbers are listed below and the days since launch at the top. The smooth line is the approximate mean spin period for the ten-orbit intervals. Since the time span of the curve has been deliberately compressed in order to fit into the figure, it appears as if the spin period is varying considerably. Actually, if this curve is shown in its proper

time perspective, the station to station variations are less than 1/4 second in a given orbit and the orbit to orbit variations or changes are within one-half of a second at most.

Another set of information which will be consolidated shortly is that data from which the pointing direction of the satellite spin axis will be determined.

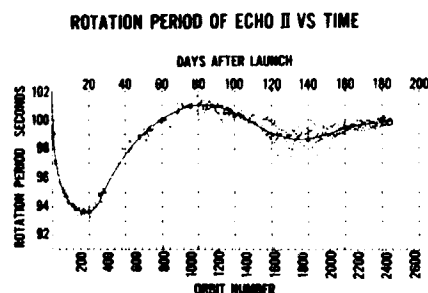


Figure 14

What is interesting is the source of information that led to the rotation period and spin axis data. This is the behavior of the beacons as the operating supply voltage varies. The supply voltage began to vary very soon after the orbit injection because the battery voltage dropped below the regulation level and its capacity dropped below the recovery point, with the result that the beacon operation became dependent on solar power. Interestingly enough, what caused these power supply changes is the rotation of the balloon itself.

The subcarrier stability was first affected by the power supply changes. For example, IRIG channels 2 and 3 (the temperature sensors) would shift two or three cycles when the supply voltage dropped below the regulation level of 19.2 volts. The frequency would then hold there until the supply voltage dropped to about 14 volts when both subcarriers quit operating. However, IRIG 4 (the pressure sensor) which contained the constant current heating device would continue to shift frequency steadily until the supply voltage dropped to 14 volts; then it would also quit. The carrier oscillator on the otherhand would shift frequency with supply voltage also, but it would not quit oscillating until the voltage dropped to about 10 volts.

Figure 15 shows a typical carrier frequency shift as a function of beacon temperature and supply voltage. Interesting enough, in the flight

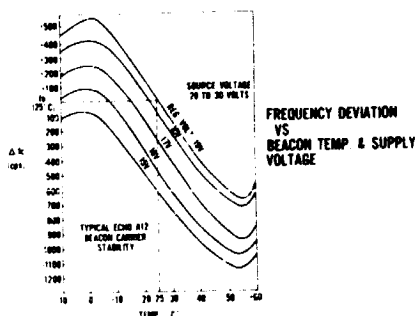


Figure 15

units the carrier frequency remained within the receiver bandwidth and would continue to be received by the tracking stations but without any subcarrier signal during a part of a rotation period and during parts of an entire pass at times. Normally one would depend on the carrier level or the AGC level to determine the spin rate but in this instance it was more advantageous to

use the subcarrier shifts since they were purely dependent on the solar cell voltage which in turn is a function of the incident illumination angle. But on the other hand, data have been obtained during some of the passes over certain stations in which the subcarrier from one beacon is present continuously for three to four rotations or about seven minutes, while another beacon signal fades in and out with the rotation period. These items should be of interest to experimenters who are monitoring the Echo II telemetry beacons.

Figure 16 shows the carrier frequency versus time as the satellite passed over the Blossom Point, Maryland tracking station at 1400 hours UT on April 17. The smooth curve is the predicted doppler shift for this pass. It is based on a nominal carrier frequency of 136.170 Mcs. The other, rollercoaster type curve is the actual frequency shift detected as the satellite passed over the station. One can see several interesting events taking place. First, there is the relative stability of the carrier during portions of the pass. Next there is the repetition of the ups and downs, which in this case occurs at 100 second intervals. Finally, the signal dropouts as the antenna pattern passed out of range or the solar power dropped to point such that the carrier quit. The beacon stability with adequate operating supply voltage is attested to by the near superposition of the two curves. The actual shift is based on the carrier frequency of 136.170,395 Mcs, which was the last check made on this beacon

before flight. The dotted portions of the curves indicate the missing signals and have been approximated.

The subcarrier data on strip charts recorded at five millimeters per second speed show these details much more clearly. However, they are not suitable for illustrations. The details will not be noticeable when reduced in size. It is regretted that they cannot be shown.

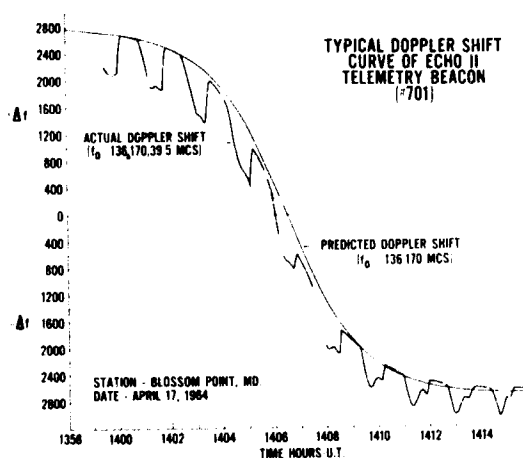


Figure 16

This concludes the report on the Echo II beacon telemetry instrumentation. In conclusion, the Project wishes to extend its acknowledgment to the numerous people who have participated in the Echo II telemetry program for their excellent effort and cooperation. Their participation has ensured a highly successful data source aboard the Echo II satellite.

#### REFERENCES

1. NASA TN D-504, "A Thermistor Pressure Gage" by J. Ainsworth and A. P. Flanick (GSFC), Nov., 1960.
2. NASA, GSFC Publication A12-0-102, Echo A12 Environmental Qualification Test Specification for Beacon-Telemetry Subsystem, dated Dec. 19, 1961 with revisions through June 28, 1962.
3. NASA, GSFC Publication A12-0-202, Echo A12 Environmental Acceptance Test Specification for Beacon-Telemetry Subsystem, dated Dec. 19, 1961 with revisions through June 28, 1962.
4. NASA, GSFC Publication A12-0-362, Performance Specification for Beacon-Telemetry Subsystem-Echo A12, dated Dec., 1961, with revisions through June 28, 1962.